ICRR-Report-484-2002-2

Detecting Very High Energy Neutrinos by the Telescope Array

Makoto Sasaki [1] Yoichi Asaoka [2] Masashi Jobashi [3]

Institute for Cosmic Ray Research, University of Tokyo, 5-1-5 Kashiwanoha, Kashiwa 277-8582, Japan

Abstract

We present the cosmic neutrino detecting potential of the Telescope Array for quasi-horizontally downward and upward air showers initiated by very high energy neutrinos penetrating the air and the Earth respectively. We adopted model predictions for extraterrestrial neutrino fluxes from active galactic nuclei, gamma-ray bursts, Greisen photo production, the collapse of topological defects, and Z-bursts. The Telescope Array, using a large array of bright and wide field-of-view fluorescence telescopes, can explore these very high energy cosmic neutrino sources.

Key words: Telescope Array, very high energy neutrino, deeply penetrating air shower, Earth skimming tau neutrino, GZK mechanism,

1 Introduction

The detection of very high energy cosmic neutrinos is important from at least three points of view. First, they can carry astrophysical information about point sources which are optically thick at almost all wavelengths and relics of an early inflationary phase in the history of the universe. Second, the connection between the emission of cosmic nuclei, gamma rays, and neutrinos from astrophysical accelerators is of considerable interest with regards the problem of the origin of extragalactic extremely high energy cosmic rays. Third, due to vacuum oscillations, a flux of high energy cosmic neutrinos is expected to be

[1] sasakim@icrr.u-tokyo.ac.jp
[2] asaoka@icrr.u-tokyo.ac.jp
[3] jobashi@icrr.u-tokyo.ac.jp

almost equally distributed among the three flavors due to vacuum oscillations, provided that the neutrinos are produced by distant objects such as gamma ray bursts (GRBs) and active galactic nuclei (AGN), and hence the study of oscillation effects on high energy neutrino fluxes can be used to study neutrino mixing and distinguish between different mass schemes [1].

In this paper we present the potential of the Telescope Array (TA), which will be able to detect cosmic neutrinos with energies above 10^{16} eV, so far unobserved. They have great potential as probes of astrophysics and particle physics phenomena. They have escaped from regions of dense matter and point back to their sources and they provide a unique window into the most violent events in the universe. Hadrons are accelerated to extremely high energies, regardless of their source, accelerating mechanism, and composition (i.e. pp and/or $p\gamma \rightarrow \pi^{\pm}$), and a subsequent decay of accompanying pions is expected to result in neutrino fluxes through the decay process $\pi \rightarrow \mu + \nu_{\mu} \rightarrow e + \nu_e\nu_{\mu} + \nu_{\mu}$, with a resultant ratio ν_{μ}/ν_e=2. Observations [2–4] of cosmic rays with energies beyond the Greisen-Zatsepin-Kuzmin (GZK) cutoff [5,6] raise interest in extremely high energy neutrinos. The GZK mechanism can lead to neutrino fluxes well above those from proposed exotic sources for the super-GZK events around the energy of 10^{18} eV.

A curious coincidence between the energy flow of the highest energy cosmic rays and gamma ray bursts (GRB) suggests a possible common source [7]. Another speculation is that very high energy cosmic rays may be the result of the annihilation of topological defects left over from the early universe [8,9]. The energy scales of such events are of the order of 10^{24} eV (GUT scale). In addition to these ideas is the proposal that the highest energy cosmic rays are evidence for novel particle physics or astrophysics [10]. These super-GZK events provide motivation for examining and confirming predictions of modes of photo production mechanisms. The neutrino fluxes of some representative sources and the range of atmospheric neutrino background as the zenith angle changes from 0° and 90° are given in Fig.1. Note the atmospheric neutrino background [21] appears to have so large spectral index that it cannot largely contribute to the neutrino detection in the higher energy region above 10^{16} eV in any source models. In each of these source cases, neutrino induced air-showers penetrate the atmosphere to a great depth. The imaging technique used in the TA detector has an advantage in this respect as it can observe the slant depth of a deeply penetrating air-shower.

The recent discovery of near-maximal ν_e-ν_{μ} and ν_{μ}-ν_{τ} mixing [11] has a significant impact on the detection strategy. The proposed astrophysical sources produce predominantly ν_{μ} and ν_e with very small admixtures of ν_{τ}. However, these sources are so far away that, even at the high energies of interest here, cosmic neutrino fluxes with a $\nu_e : \nu_{\mu} : \nu_{\tau}$ ratio at the source of $1 : 2 : 0$, inevitably oscillate in the three neutrino framework to a ratio of $1 : 1 : 1$,

irrespective of the mixing angle.

By looking for upward moving showers from Earth-skimming tau neutrinos, one can test for the existence of neutrino oscillations [12,13]. Once created in the Earth, a charged lepton loses energy through Bremsstrahlung, pair production, and photonuclear interactions. At the Earth's surface, with a density of about 2.7 g/cm^3, tau leptons and muons are expected to travel 11 km and 1.5 km, respectively, before losing a decade in energy; electrons however do not travel any significant distance. Detectable neutrinos therefore skim the Earth at angles approximately 1° above the horizontal and these events are expected to be predominantly showers induced by tau neutrinos.

Another important signature of very high energy tau neutrinos is the "double bang" which they produce in the atmosphere. The initial shower is produced by the original interaction which creates a tau lepton and a hadronic shower. This is followed by the decay of the tau lepton, producing the second shower bang. The two bangs are separated by a distance of ∼4.9 km ($E_\tau/10^{17}$ eV)

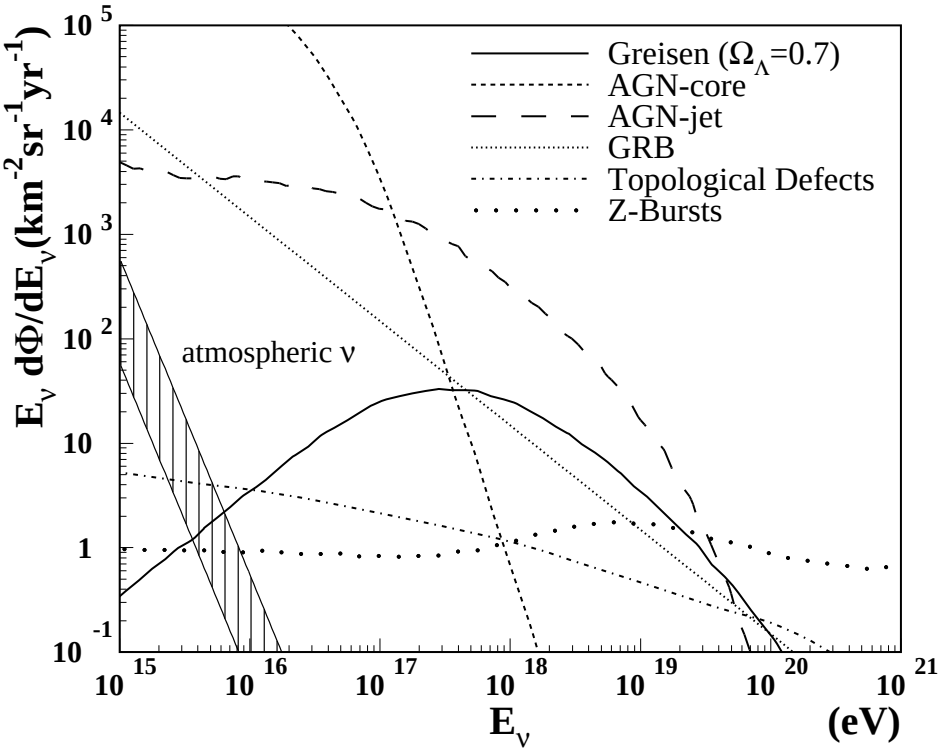

Fig. 1. Differential fluxes of muon neutrinos ($\nu_\mu + \bar{\nu}_\mu$) from Greisen photo production [14], active galactic nuclei [16,15], gamma ray bursts [7], topological defects [17], and Z-bursts [18]. An AGN-core flux model [19] has been rejected by AMANDA-B10 [20]. The band with vertical hatching shows the range of atmospheric neutrino background [21] as the zenith angle changes from 90° (highest) to 0° (lowest).

where E_τ is the energy of the tau lepton converted from the tau neutrino. This decay length is measurable with the imaging telescopes in the TA detector.

2 The TA Detector

The TA detector (Figs.2 and 3) has been designed in order to investigate the origin of the highest energy cosmic rays [22,23]. For this purpose, the detector is required to obtain statistics of a much greater number of events than the rate of one super-GZK event per year that the AGASA is able to detect. It should also provide particle identification as well as accurate determination of the direction of the primary cosmic ray to test the source models at a high confidence level. The basic measurement principle use a huge effective aperture to detect the image of fluorescence light produced by air showers and from this the longitudinal shower development can be reconstructed.

The TA detector consists of 10 observational stations installed over an area at about 30-40 km intervals as shown in Fig. 2. Each station consists of 40 telescopes with a 3 m-diameter f/1 mirror system on 2 layers of supports. 256 2-inch photo multiplier tubes (PMTs) mounted on the focal plane serve as pixels of the fluorescence sensor of each telescope. Each PMT covers a visual field of angular aperture $1.1^\circ \times 1.0^\circ$. We expect the detection rate by the TA detector for events with energies beyond the GZK-cutoff to exceed that of AGASA by about 30 times. We note that this is similar to that expected for another proposed detector, the Pierre Auger Observatory (AUGER) [24]. The accuracy of determining the energy and arrival direction for the highest energy events are roughly 25% and 0.6° respectively.

In order for the detector stations to have good visibility, atmospheric transparency, no significant nearby sources of light pollution, and be away from significant traffic, it is preferable to install them on top of small mountains or hills, while still maintaining the arrangement in 30-40 km intervals. We have identified sites in the south-west area of Delta in southern Utah. The planned detector station array covers an area of 200 km^2.

3 Neutrinos Deeply Penetrating the Atmosphere

Neutrinos can produce air showers through interactions with the atmosphere. The number of the shower depends on the particular interaction. We consider here both inelastic charged and neutral current interactions, which always produce hadronic showers. Note however that the case of charged current electron

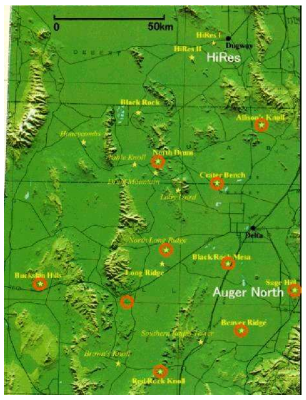

Fig. 2. TA site arrangement.

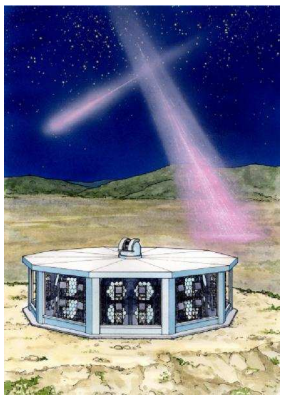

Fig. 3. TA detector station.

neutrino interactions, in addition to the emerging electron, a pure electromagnetic shower carrying a large fraction of the incoming particle energy is produced.

In our discussions of neutrino induced showers we make use of new calculations of the cross sections of charged-current and neutral current interactions of neutrinos with nuclei [28,25], according to the CTEQ4-DIS (deep inelastic scattering) parton distributions [29]. The CTEQ4-DIS parton distributions take account of new information about parton distributions within the nucleon [30] using accurate and extensive DIS data from the New Muon Collaboration (NMC) [31] and DESY ep collider HERA [32,33], as well as new data from E665 [34].

For a neutrino flux dI_ν/dE_ν interacting through a particular process with differential cross section $d\sigma/dy$, where y is the fraction of the incident particle energy transferred to the target, the event rate for deeply penetrating showers can be obtained by a simple convolution:

$$Rate[E_\nu > E_{th}] \; = \; N_A \rho_{air} \int_{E_{th}}^{\infty} dE_\nu \int_0^1 dy \frac{dI_\nu}{dE_\nu}(E_\nu) \frac{d\sigma}{dy}(E_\nu, y) \epsilon(E_{sh}),$$

where N_A is Avogadro's number and ρ_{air} is the air density. The energy integral corresponds to the primary neutrino energy E_ν which is related to the shower energy E_{sh}, the relationship being different for each interaction. ϵ is the detector acceptance, a function of shower energy, which corresponds to the volume and solid angle integrals for different shower positions and orientations with respect to the detector. The function is different for both showers induced by charged current electron neutrino interactions and those arising in neutral current or muon neutrino interactions. This is because hadronic and electromagnetic showers have different particle distribution functions. For $(\nu_e + \overline{\nu}_e)N$ charged current interactions, we take the shower energy to be the sum of hadronic and electromagnetic energies, $E_{sh} = E_\nu$. For $(\nu_\mu + \overline{\nu}_\mu)N$

charged current interactions and for neutral current interactions, we take the shower energy to be the hadronic energy, $E_{sh} = yE_\nu$. We take the inelasity y to be a function of E_ν as in reference [25], while $< y > \sim 0.25$ does not depend strongly on the primary energy beyond 10^{16} eV in both charged and neutral current interactions.

In the case of ν_τ, we must also take into account the decay length of secondary tau leptons, subsequent tau lepton decay, and a further energy input into the air shower from decaying electrons, photons, and hadrons. The tau decay branching fractions and tau polarization effect are reasonably well accounted for simply by assuming that the energies of neutral mesons fully contribute to the electromagnetic showers. The adopted decay branching fractions and the momentum spectra of the decay with a polarization of ± 1 in the colinear approximation in the laboratory frame are shown in Table 1 and Fig. 4 respectively. The τ decay length is often long enough that two subsequent energy inputs into the air showers can be seen in the field of view.

Table 1
Tau decay branching fractions from Particle Data Group (PDG) [42] and used in the simulation for events in TA. The branching fractions in the simulation should include π^0 contributions.

Tau decay modes	PDG B.F. (%)	B.F. (%) in the simulation
$\tau \to \mu\nu\bar{\nu}$	17.37±0.07	17
$\tau \to e\nu\bar{\nu}$	17.83±0.06	18
$\tau \to \pi(K)\nu$	11.79±0.12	13
$\tau \to \rho\nu$	25.40±0.14	37 ($\geq$ 1 neutral)
$\tau \to a_1\nu$	9.49±0.11	15 (all 3 prongs)
$\tau \to hhh \geq \pi^0\nu$	4.49±0.08	

Simulations for a given primary cosmic ray (electron neutrino, muon neutrino, tau neutrino, and proton) were performed at fixed energies. The shower energy for neutrinos depends on the generation, as described above. For each shower energy, the mean depth of the proton shower maximum was determined from simulations [35]. For each primary particle at each energy, the mean of the interaction length X_1 was determined from the above interaction cross sections of neutrinos with nuclei or of protons, X_1=83.1$(E/\mathrm{GeV})^{-0.052}$ g/cm^2 [36]. The shower energy determines the shower size at a maximum, N_{max}[37]. Given N_{max}, a slant depth at the maximum shower size X_{max}, and X_1, the complete longitudinal profile can be described by the Gaisser-Hillas function [38]. The Nishimura-Kamata-Greisen (NKG) lateral distribution function [39,40] normalized with the Gaisser parameterization has been used to find the total number of electrons and positrons in hadronic (electromagnetic) cascade showers in order to determine the location where fluorescence is produced.

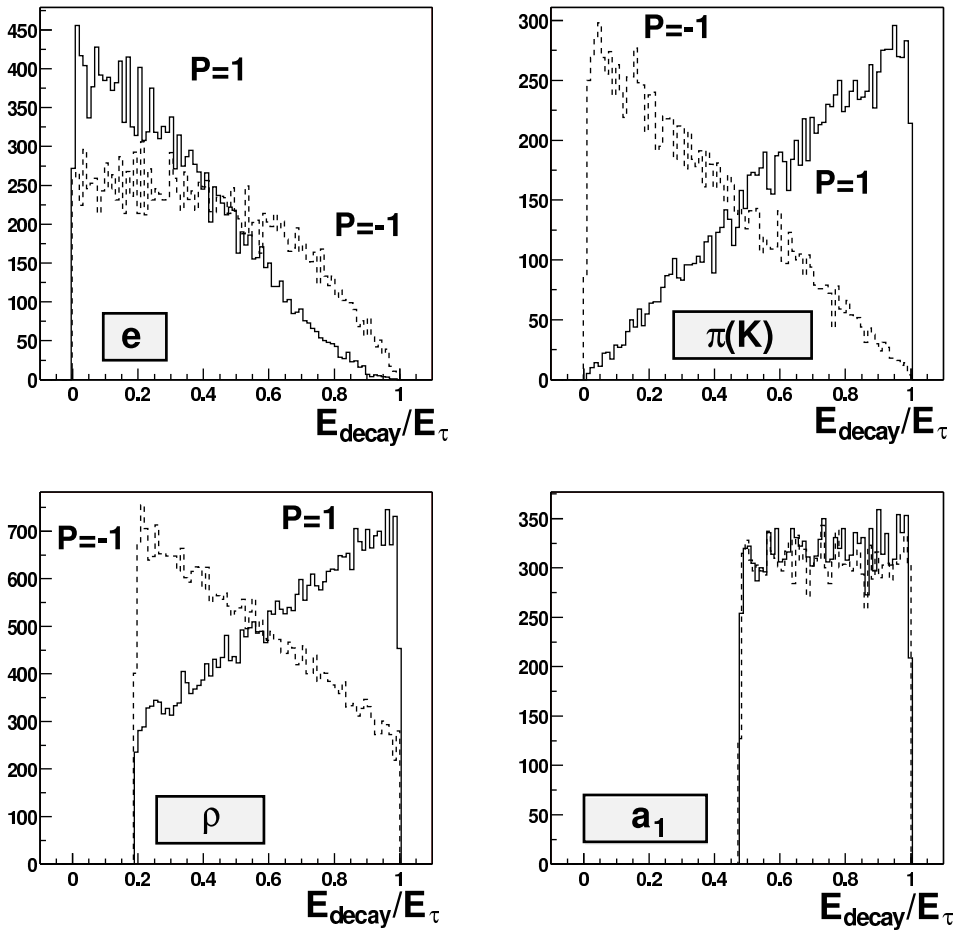

Fig. 4. Distributions in visible decay energy divided by E_τ corresponding to values of tau polarization +/- 1 for $\tau \to e\nu\bar{\nu}$, $\tau \to \pi(K)\nu$, $\tau \to \rho\nu$, and $\tau \to a_1\nu$.

In our simulations we took into account the fluctuations of the first interaction depth, impact point, and directional angles of air shower cores, with appropriate distributions, but not air shower size fluctuations.

An important factor that must be calculated is the light yield arriving at the detector site. For this the Rayleigh and Mie scattering processes were simulated, with full account taken of the spectral characteristics of the light. The isotropically emitted fluorescence light, as well as direct and scattered Cerenkov light, is propagated, and the night sky background noise was added to the signal. All processes that affect the overall optical efficiency, mirror area and reflectivity, optical filter transmission, and PMT quantum efficiency factors were included in the light spectrum to give the photoelectron yield in each PMT, due to both signal and noise.

A "fired" PMT is defined such that its instantaneous photoelectron current is greater than the 4σ noise level of the night sky background. We preselected events such that at least one of the 10 stations contains at least 6 firing PMTs. To ensure track quality, we cut events for which shower maxima were

not viewed by any station. Finally, to reject proton background events, we selected only events with $X_{max} > 1700$ g/cm^2. Once the selection cuts were made the detector aperture could be determined and the acceptances calculated by multiplying the appropriate interaction length of a neutrino with a nucleon. Figure 5 shows the shower slant depth distributions from Monte Carlo simulations by which neutrino events can be distinguished from proton events. The results are shown in Fig. 6 for electron, muon, and tau neutrinos as a function of the primary energy. The acceptances of the TA for high-energy neutrinos deeply penetrating air compare well with those of IceCube and AUGER [26,25,27] in lower and higher energy regions respectively, even if we take into account the 10 % duty factor of TA, which is a rate of the observation time at moonless night in good weather.

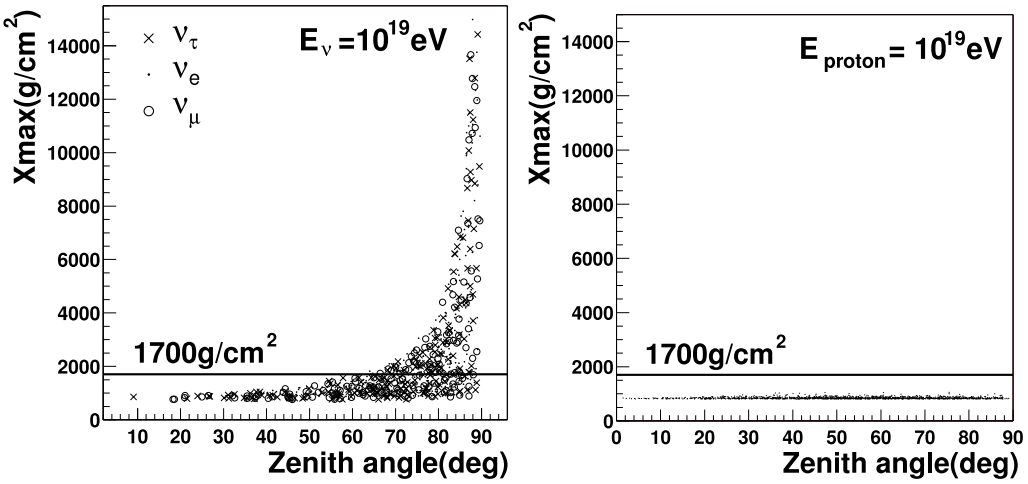

Fig. 5. Shower slant depth distributions for neutrino (*left*) and proton (*right*) induced events with energies of 10^{19} eV from Monte Carlo simulations showing the cut of 1700 g/cm^2, by which neutrino events can be distinguished from proton events.

4 Earth-skimming Tau Neutrinos

Very high energy neutrinos penetrate the Earth and convert to charged leptons which then travel through the Earth. This sequence is illustrated for an event with a nadir angle θ in Fig. 7. We define the critical angle θ_c such that the chord thickness at the nadir angle θ_c corresponds to the charged current interaction length $L^{\nu}_{CC}(E_\nu)$ determined by the interaction cross section for a neutrino traveling with energy E_ν. For nadir angles smaller than θ_c, neutrinos are shadowed by the Earth, and for larger nadir angles, they rarely interact to produce charged leptons. Table 2 shows charged current cross sections, interaction lengths, and $90^\circ - \theta_c$ at various neutrino energies. For neutrino energies above 10^{17} eV, $90^\circ - \theta_c$ is small and both the neutrinos and the created leptons travel essentially horizontally.

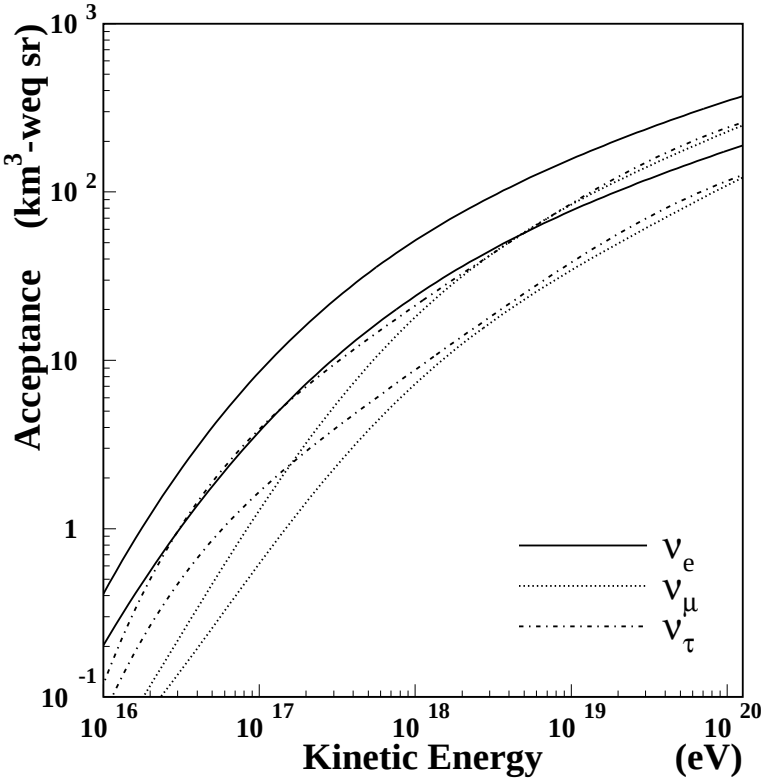

Fig. 6. Acceptance of the TA detector (1 stations) to a neutrino induced air shower. Volume units are km^3 of water equivalent. The higher and lower curves correspond to events after preselection and proton rejection cuts respectively.

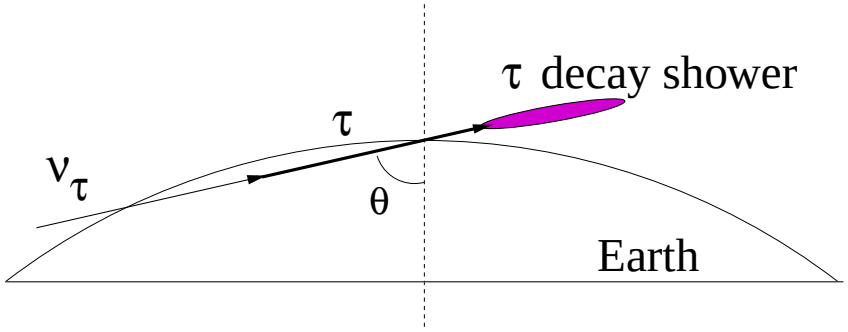

Fig. 7. A schematic picture of Earth-skimming tau neutrino events.

Once created, a charged lepton loses energy through Bremsstrahlung, pair production, and photonuclear interactions. Electrons lose their energy too quickly in the Earth and hence cannot be detected by fluorescence. Assuming that a lepton loses energy uniformly and continuously, its energy loss can be parametrized by: $dE_l/dz = -\beta_l \rho E_l$, where the Earth's density ρ can be simplified to be 2.65 g/cm^3 uniformly for small nadir angles. The values of the constant β_l are $\beta_\mu \sim 6.0 \times 10^{-6} cm^2/g$ and $\beta_\tau \sim 0.8 \times 10^{-6} cm^2/g$ for muons and tau leptons respectively for the energies of interest here [41]. Hence, at the Earth's surface muons and tau leptons can travel 1.5 km and

Table 2
Charged current (CC) cross sections, interaction lengths and $90^\circ - \theta_c$ (see text) for νN interactions for the CTEQ-DIS distributions [25].

E_ν (eV)	σ^ν_{CC} (10^{-33} cm^2)	L^ν_{CC} (10^7g/cm^2)	$90^\circ - \theta_c$ ($^\circ$)
10^{16}	1.8	94	16
10^{17}	4.8	35	5.9
10^{18}	12	14	2.3
10^{19}	30	5.5	0.89
10^{20}	71	2.4	0.35

11 km, respectively, before losing a decade in energy. Therefore, tau neutrinos contribute dominantly to Earth-skimming events observed above the Earth's surface. Figure 8 shows distributions on the plane of energy E_τ and $90^\circ - \theta$ of tau leptons that exit the Earth from primary neutrinos with energies of 10^{19} eV and 10^{17} eV.

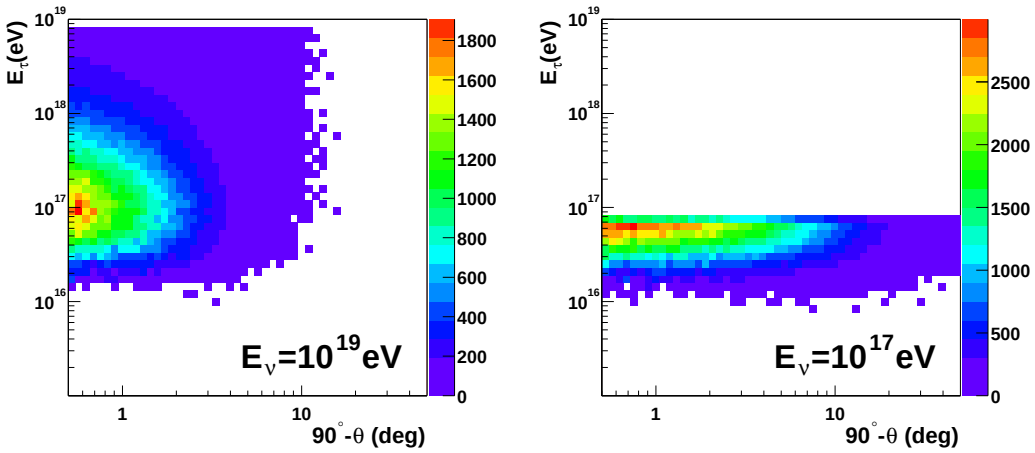

Fig. 8. Distribution on the plane of energy E_τ and $90^\circ - \theta$ of tau leptons that exit the Earth in the case of a primary neutrino energy of 10^{19} eV (*left*) and 10^{17} eV (*right*).

The survival probability P_{svv} for a tau losing energy as it moves through the Earth is described by the energy loss dE_τ/dz as above, and

$$\frac{dP_{svv}}{dz} = -\frac{P_{svv}}{c\tau_\tau E_\tau/m_\tau} \quad ,$$

where c is the speed of light and m_τ and τ_τ are tau lepton's rest mass and lifetime respectively. These can be solved and the survival probability given by

$$P_{svv} = \exp\left[\frac{m_\tau}{c\tau_\tau\beta_\tau\rho}\left(\frac{1}{E_\nu} - \frac{1}{E_\tau}\right)\right] \quad .$$

For tau leptons, this factor plays a significant role. The competition between L^{ν}_{CC} and P_{svv} makes the peak of the distribution at the survived tau lepton energy of 10^{17} eV in Fig. 8, which is independent of the primary tau neutrino energy. Due to this effect, lower energy sensitivity of an air fluorescence telescope makes a key role to detect the Earth skimming tau neutrinos.

The flux of survived taus with energy $E_{min} < E_{\tau} < E_{max}$ is

$$\Phi_{\tau} = \frac{ln(E_{max}/E_{min})}{2R\beta_{\tau}\rho}\Phi_{\nu} \quad ,$$

where Φ_{ν} is the flux of neutrinos. As a result, the flux in any given decade in tau energy is $\Phi_{\tau} = 8.5 \times 10^{-4}\Phi_{\nu}$, that is, 1 in every 1200 neutrinos that skims the Earth emerges as a tau lepton with the required energy [12]. This remarkably simple and robust statement is quite useful because it is independent of the neutrino energy and microscopic details. We have examined our Monte Carlo simulation results by comparison with this analytic estimate.

The tau decay length is given by $L_{\tau} = c\tau_{\tau}(E_{\tau}/m_{\tau}) \sim 4.9$ km $(E_{\tau}/10^{17}$ eV) , using the lifetime $c\tau_{\tau} = 87.11$ μm the tau mass $m_{\tau} = 1777.03$ MeV from PDG [42]. The complete treatment for tau decays can be performed as described in the previous section. Effective detection apertures and acceptances have been estimated for Earth-skimming tau events changing the neutrino energies from the detailed Monte Carlo simulation. Figure 9 shows the effective detection acceptances using only one TA station. The tau decay length as a function of the tau lepton energy which is observed within the view of the telescope makes the detection acceptance slightly decrease as increasing the kinetic energy of Earth skimming tau neutrino above the primary energy of 10^{19} eV.

5 Detection Event Rates

Models that assumes shock acceleration in the Active Galactic Neuclei (AGN) cores predict relatively flat fluxes up to energies of about 10^{15} eV [15]. The GeV to TeV gamma ray emissions observed in AGN corresponds to the blazar class. Most recent models for the proton blazars site the acceleration in the jets themselves. We use the prediction of reference [16], which illustrates that the emitted neutrinos may extend well into the EeV region. Annual event rates have been calculated for the TA detector for neutrino induced air showers with fluxes from GRB model [7] and Greisen neutrino [14] models as well as from AGN-core [15] and AGN-jet [16], assuming a duty cycle of 10%, and are shown in Table 3. The testability of the bottom-up scenario models is statistically simple even when considering only shower events deeply penetrating the air.

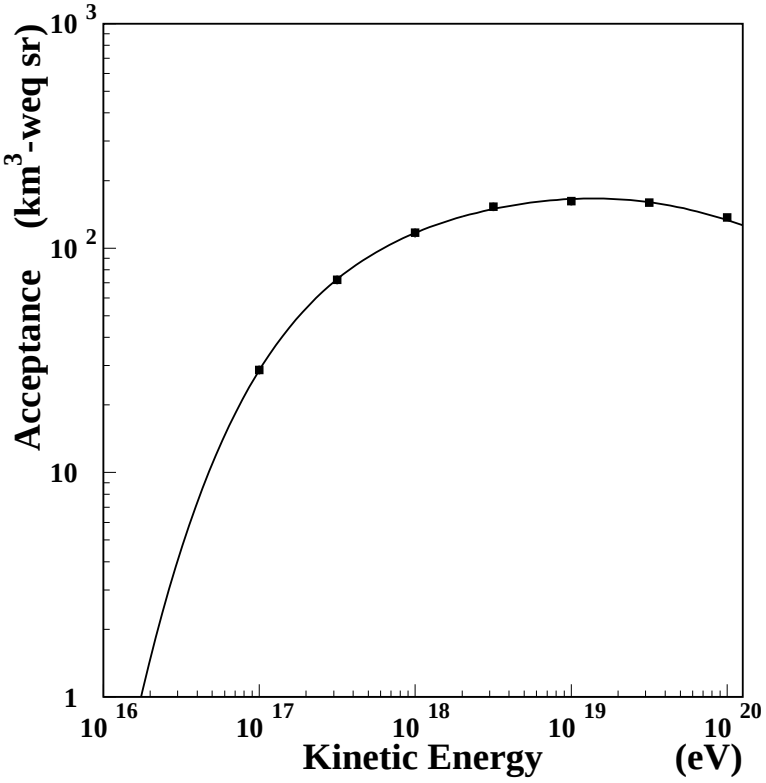

Fig. 9. Detection acceptance estimate (in km^3-water-equivalent steradian) for Earth-skimming tau leptons through their decays to electromagnetic and/or hadronic air showers with only one TA detector station.

We also compare the detectability of Earth-skimming tau neutrino events with the downward events described above. Table 3 also lists annual event rates for neutrino induced air-showers from various models including top-down scenario sources of shower events deeply penetrating the air and Earth-skimming events. The duty factor of 10% is assumed as usual. The enhancement of the statistics by considering Earth-skimming events is significant, particularly in the ultra-high energy region. Hence it is feasible to test the top-down scenario models such as topological defects and Z-bursts in a statistically significant way by considering both downward and upward neutrino-induced air-shower events in complementary energy regions.

6 Conclusions

The next generation of cosmic ray detectors such as AUGER and the TA have target volumes of atmosphere competitive with or better than that of IceCube and their annual detection rates assuming AGN-jet proton acceleration models are statistically sizable [26,27]. The TA using an air fluorescence technique is advanced as a method for discriminating primary neutrinos proton induced

Table 3
Annual event rates in the TA detector for neutrino induced air showers with fluxes from AGN-core [15], AGN-jet [16], GRB model [7], Greisen neutrino [14], topological defects [17], and Z-bursts [18] models (see text). A duty factor of 10% was assumed.

	CCν_e	CCν_μ	CCν_τ	NC	ESν_τ	Total
AGN-core	8.9	1.4	4.2	1.7	3.1	19.3
AGN-jet	6.8	2.4	3.4	3.1	42.8	58.4
GRB	0.48	0.17	0.25	0.22	2.48	3.60
Greisen	0.52	0.25	0.30	0.32	3.21	4.59
TD	0.09	0.06	0.06	0.07	0.34	0.63
Z-Bursts	0.46	0.33	0.34	0.40	1.19	2.72

air showers. Recently a novel strategy for detecting Earth-skimming extremely high energy neutrinos has been quantitatively proposed for which significant improvements in detection can be made using the TA detector compared to down-going neutrino detection [12]. Encouragingly, extremely high energy cosmic neutrino sources, to say nothing of AGN proton acceleration models, such as Greisen photo production [14], topological defects [17], long-lived super heavy particles, and Z-bursts [18], may be experimentally tested with the TA.

7 Acknowledgments

We are indebted to my colleagues in the TA Collaboration, especially those who have contributed to the TA Design Report, for assistance in the preparation of this paper. We would like to especially acknowledge the contributions of Prof. T. Matsuda and Prof. C. Fukunaga for useful discussions.

References

[1] H. Athar, M. Jezabek and O. Yasuda, Phys. Rev. D62 (2000) 103007.

[2] M. Takeda et al., Phys. Rev. Lett. **81** (1998) 1163.

[3] J.D. Bird et al., Phys. Rev. Lett. **71** (1993) 3401.

[4] B.N. Afanasiev et al., Proc. 24th ICRC, Roma, **2** (1995) 756.

[5] K. Greisen, Phys. Rev. Lett. **16** (1966) 748.

[6] G.T. Zatsepin and V.A. Kuzmin, JETP Letters **4** (1966) 78.

[7] E. Waxman, Phys. Rev. Lett. **75** (1995) 386.

[8] C.T. Hill, D.N. Schramm and T.P. Walker, Phys. Rev. **D36** (1987) 1007.

[9] P. Bhattacharjee, C.T. Hill and D.N. Schramm, Phys. Rev. Lett. **69** (1992) 567.

[10] D. Fargion, D.Salis, Proc. 25th ICRC, **2**, 153 (Durban, 1997); T. J. Weiler, Astropart. Phys. **11**, 303 (1999); D. Fargion, B. Mele, and A. Salis, Astrophys. J. **517**, (1999) 725.

[11] S. Fukuda et al (Super-Kamiokande Collaboration), Phys. Rev. Lett. **86** (2001) 5656.

[12] J.L. Feng, P. Fisher, F. Wilczek, and T.M. Yu, Phys. Rev. Lett. **88** (2002) 161102.

[13] D. Fargion, Astrophys. J. **570**, (2002) in press; D. Fargopm, arXiv:hep-ph/0111289.

[14] R. Engel, D. Seckel, and T. Stanev, Phys. Rev. **D64** (2001) 093010.

[15] F.W. Stecker, M.H. Salamon, Space Sci.Rev. 75 (1996) 341-355.

[16] K. Mannheim, Astropart. Phys. **3** (1995) 295.

[17] G. Sigl, et al., Phys. Lett. **B392** (1997) 129.

[18] S. Yoshida, G. Sigl and S. Lee, Phys. Rev. Lett. **81** (1998) 5505.

[19] A.P. Szabo and R.J. Protheroe in Proc. High Energy Neutrino Astrophysics Workshop (U. Hawaii. March 1992), ed. V.J. Stenger, J.L. Learned, S. Pakvasa and X.Tata, World Scientific, 1993, p.24.

[20] AMANDA collaboration, J.Ahrens, *et al.*, astro-ph/0206487, submitted to Phys. Rev. D.

[21] L.V. Volkova, et al., Phys. Atom. Nucl. **64** (2001) 266.

[22] M. Sasaki, Proc. 25th ICRC, **5**, 369 (Durban, 1997).

[23] The Telescope Array Project: Design Report, http://www-ta.icrr.u-tokyo.ac.jp; M. Sasaki, Proc. of the EHECR2001, ICRR-Report-481-2001-11 (2001).

[24] The Pierre Auger Project: Design Report, 2nd ed. March 1997, http://www.auger.org/.

[25] R. Gandihi, C. Quigg, M. H. Reno, and I. Sarcevic, Astropart. Phys. **5** (1996) 81.

[26] M. Sasaki: Proc. the 1st workshop on *Neutrino Oscillations and their Origin*, (2000) 79.

[27] K.S. Capelle, J.W. Cronin, G. Parente and E. Zas: Astropart. Phys. **8** (1998) 321.

[28] R. Gandihi, C. Quigg, M. H. Reno, and I. Sarcevic, Phys. Rev. D **58**, 093009 (1998).

[29] CTEQ Collaboration, H. L. Lai *et al.*, Phys. Rev. D **55** 1280 (1997).

[30] C. Quigg, FERMILAB-CONF-97/158-T.

[31] NMC, M. Arneodo *et al.*, Phys. Lett. B **36** 471 (1995).

[32] H1 Collaboration, S. Aid *et al.*, Nucl. Phys. B **439** 471 (1995); Nucl. Phys. B **470** 3 (1996).

[33] ZEUS Collaboration, M. Derrick *et al.*, Z. Phys. C **65** 379 (1995).

[34] E665 Collaboration, M. R. Adams *et al.*, Phys. Rev. D **54**, 3006 (1996).

[35] T. K. Gaisser *et al.*, Phys. Rev. D **47**, 1919 (1993).

[36] M. Honda *et al.*, Phys. Rev. Lett., **70**, 525 (1993).

[37] R. M. Baltrusitis *et al.*, Proc. 19th ICRC, La Jolla, **7** (1985) 159.

[38] T. K. Gaisser and A. M. Hillas, Proc. 15th ICRC (Plovdiv) **7** (1977) 353.

[39] K. Kamata and J. Nishimura, Prog. Theor. Phys. Suppl. **6**, 93 (1958).

[40] K. Greisen, Prog. Cosmic Ray Physics **3**, 1 (1956).

[41] P. Lipari and T. Stanev, Phys. Rev. **D44** 3543 (1991).

[42] Particle Data Group (D.E. Groom *et al.*) Eur. Phys. J. **C15**, 1-878 (2000).